Automated Wildfire Detection Through Artificial Neural Networks

Jerry Miller (NASA), Kirk Borne (GMU), Brian Thomas (UMD), ☒
Zhenping Huang (UMD), and Yuechen Chi (GMU)

Abstract: We have tested and deployed Artificial Neural Network (ANN) data mining techniques to analyze remotely sensed multi-channel imaging data from MODIS, GOES, and AVHRR. The goal is to train the ANN to learn the signatures of wildfires in remotely sensed data in order to automate the detection process. We train the ANN using the set of human-detected wildfires in the U.S., which are provided by the Hazard Mapping System (HMS) wildfire detection group at NOAA/NESDIS. The ANN is trained to mimic the behavior of fire detection algorithms and the subjective decision-making by NOAA HMS Fire Analysts. We use a local extremum search in order to isolate fire pixels, and then we extract a 7x7 pixel array around that location in 3 spectral channels. The corresponding 147 pixel values are used to populate a 147-dimensional input vector that is fed into the ANN. The ANN accuracy is tested and overfitting is avoided by using a subset of the training data that is set aside as a test data set. We have achieved an automated fire detection accuracy of 80-92%, depending on a variety of ANN parameters and for different instrument channels among the 3 satellites. We believe that this system can be deployed worldwide or for any region to detect wildfires automatically in satellite imagery of those regions. These detections can ultimately be used to provide thermal inputs to climate models.

1. Introduction

Wildfires have a profound impact upon the biosphere and our society in general. They cause loss of life, destruction of personal property and natural resources and alter the chemistry of the atmosphere. In response to the concern over the consequences of wildland fire and to support the fire management community, the National Oceanic and Atmospheric Administration (NOAA), National Environmental Satellite, Data and Information Service (NESDIS) located in Camp Springs, Maryland gradually developed an operational system to routinely monitor wildland fire by satellite observations. The Hazard Mapping System, as it is known today, allows a team of trained fire analysts to examine and integrate, on a daily basis, remote sensing data from Geostationary Operational Environmental Satellite (GOES), Advanced Very High Resolution Radiometer (AVHRR) and Moderate Resolution Imaging Spectroradiometer (MODIS) satellite sensors and generate a 24 hour fire product for the conterminous United States. Although assisted by automated fire detection algorithms, NOAA has not been able to eliminate the human element from their fire detection procedures. As a consequence, the manually intensive effort has prevented NOAA from transitioning to a global fire product as urged particularly by climate modelers. NASA at Goddard Space Flight Center in Greenbelt, Maryland is assisting NOAA more fully automate the Hazard Mapping System by training neural networks to mimic the decision-making process of the fire

analyst team as well as the automated algorithms.

2. Data Archiving

Two years ago, the Computing, Information and Communications Technology (CICT), Program operating out of the Ames Research Center in Moffett Field, California, provided funding for the research effort to get underway. A team of government and (ultimately) University personnel were assembled with the intent of applying artificial intelligence techniques to NOAA's automation problem. NASA began archiving satellite imagery from GOES, AVHRR and MODIS satellite sensors in the summer of 2003. Three spectral channels for each of 3 science instruments were provided by NOAA NESDIS by uploading to a NASA computer within the Information Systems Division at Goddard Space Flight Center. The spectral bands, being only a subset of those available from each instrument were found to be the most useful in fire identification by NESDIS and are shown in Table 1. Both reflectance and brightness temperature were scaled by NESDIS to a range of 0 – 255.

Table 1. Spectral Bands Provided by NESDIS

GOES	AVHRR	MODIS
0.62 μm (ch1) 3.9 μm (ch2) 10.7 μm (ch4)	0.66 μm (ch1) 0.91 μm (ch2) 3.7 μm (ch3b)	0.66 μm (ch1) 0.86 μm (ch2) 3.96 μm (ch22)

It became apparent almost immediately that the huge volume of satellite imagery which NESDIS provided but did not archive themselves presented a formidable storage problem. Each day, NESDIS processes 96 GOES images files, 25 AVHRR image files and 16 MODIS image files which were uploaded to NASA. Satellite imagery, in Lambert Conformal Conic Projections, plus ancillary data required approximately 1.44 gigabytes of storage daily. A Mac G5 with 12 Maxtor external (250GB) disk drives was able to handle the enormous storage requirement.

2. Preliminary Analysis

The preliminary analysis consisted of a series of scatter plots starting with GOES imagery to determine separability of fire and non-fire clusters. An example is shown in Figure 1 in which clusters of background pixels (upper) and fire pixels (lower) are distinguishable in a GOES, channel 1 (reflectance) and channel 2 (brightness temperature) scatter plot for a particular pixel over the course of a single day. Intensities

are background subtracted. This was the first indication, confirmed by subsequent analysis, that different fires types (crown, surface and ground) did not have unique fire signatures and that a simple linear separability existed between the two classes of fires and non-fires.

Figure 1 Scatter Plot of GOES Channels 1 and 2

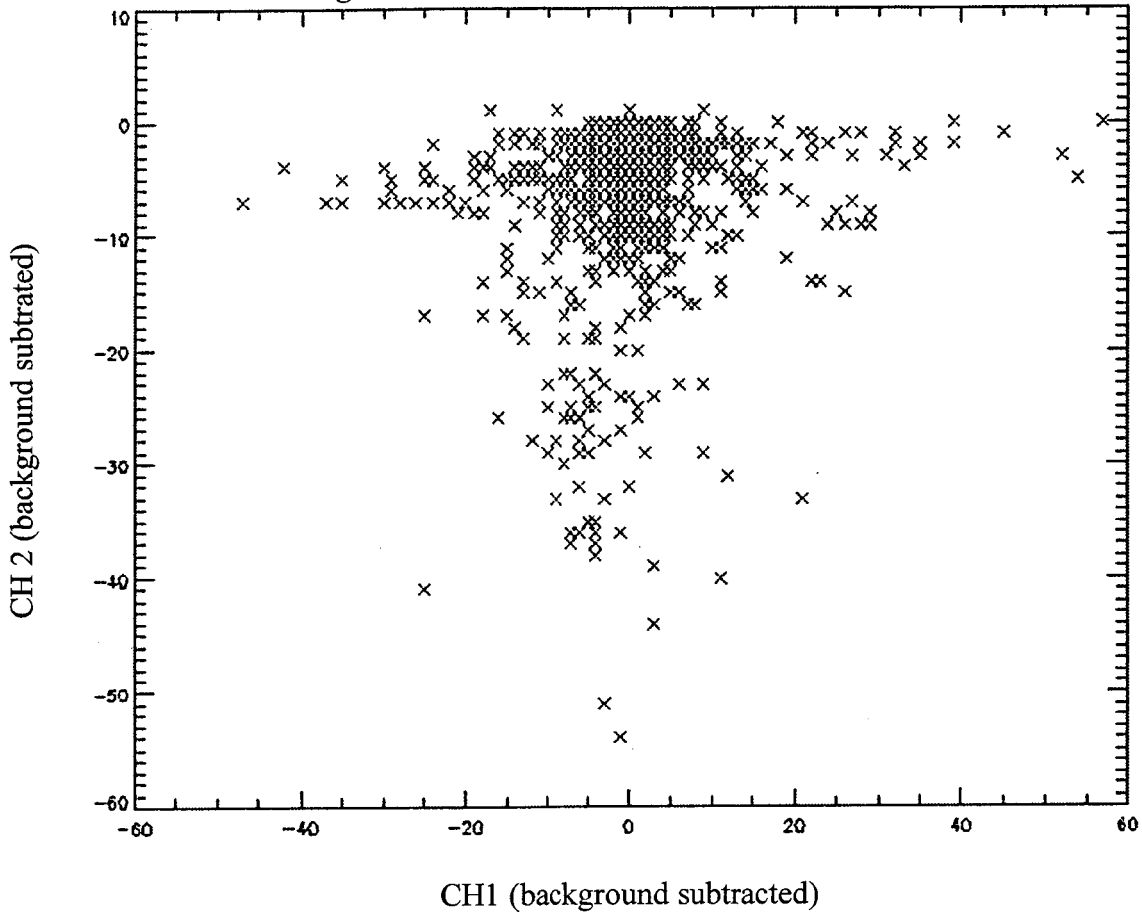

3. Data Reduction

A good deal of thought, time and attention went into the composition of adequate neural network training sets. Early attempts included time and geographic location parameters in addition to spectral information but due to subsequent difficulties in obtaining convergence, ultimately only the spectral information was used. The original guiding principle in training set composition was to use NOAA's ASCII data-formatted fire product to locate fires within satellite imagery, then extract 3-band pixel information at these points.

Table 2 depicts the appearance of NOAA's fire product in ASCII data format. As shown, on each line and for each separate fire, the geographic coordinates of the fire are followed by a time stamp, the satellite imagery from which the determination was made and finally

the method of detection which may have been a human analyst or one of the automated algorithms: Wildfire Automated Biomass Burning Algorithm (WF-ABBA) [1,2], Fire Identification Mapping and Monitoring Algorithm (FIMMA) [1,2], MODIS MOD14 [3] Fire product (MODIS).

Table 2. ASCII Data Format of NOAA Fire Product (as of 05/16/03)

Lon	Lat	Time	Satellite	Method of Detect
-80.597	22.932	1830	MODIS AQUA	MODIS
-79.648	34.913	1829	MODIS	ANALYSIS
-81.048	33.195	1829	MODIS	ANALYSIS
-83.037	36.219	1829	MODIS	ANALYSIS
-83.037	36.219	1829	MODIS	ANALYSIS
-85.767	49.517	1805	AVHRR NOAA-16	FIMMA
-84.465	48.926	2130	GOES-WEST	ABBA
-84.481	48.888	2230	GOES-WEST	ABBA
-84.521	48.864	2030	GOES-WEST	ABBA
-84.557	48.891	1835	MODIS AQUA	MODIS
-84.561	48.881	1655	MODIS TERRA	MODIS
-84.561	48.881	1835	MODIS AQUA	MODIS
-89.433	36.827	1700	MODIS TERRA	MODIS
-89.750	36.198	1845	GOES	ANALYSIS

Using a software package called Environment for Visualizing Images (ENVI), geographic coordinates were converted to pixel row and column coordinates for a particular image being processed through a series of ENVI function calls embedded in IDL code. When examining fires using ENVI in visual mode however it was found that fires were not in the precise location where the geographic coordinates placed them, being offset possibly by several pixels from their expected location. Considering the 1 kilometer spatial resolution of MODIS and AVHRR, the offset error might have been 2 or 3 kilometers but for GOES data in the thermal band (4 KM resolution) the error could have been as much as 12 kilometers. This offset was attributed to 3 sources: spacecraft navigation errors, the inherent tolerances within NOAA software and operational errors in the point-and-click method of a Fire Analyst identifying fire locations with a mouse.

One of the best clues for identifying wildfires that NOAA Fire Analysts employ is to visually inspect the 4 micron band for dark spots within NESDIS-processed satellite imagery. NOAA software has been written in such a way that brightness temperatures, which have been scaled to a range of 0 – 255 will assume the lowest values for the hottest fires. This can be seen clearly in Figure 2a. which displays a GOES Channel 2 satellite image of Northern Florida, Julian day 126 in 2003. A fire at coordinates –82.10 degrees West Longitude, 30.49 degrees North Latitude is shown (enclosed in rectangle). Although appearing to be a pinpoint location in the normal view, a zoom-in in Figure 2b. indicates that the fire is actually spread across numerous pixel locations. In order to extract the spectral information around this exemplar fire, using the approximate location

as specified by the ASCII data fire product, our software performed a local minima search in the 4 micron band in the expected region to pinpoint the hottest fire pixel (lowest intensity value). Spectral information was then collected around that image coordinate in all 3 bands.

Figure 2a. GOES CH 2
Northern Florida Fire

Figure 2b. GOES CH 2 (Zoom)
Northern Florida Fire

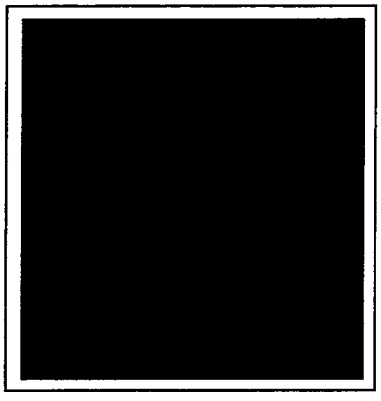

Three different methods to characterize a fire across 3 spectral bands were investigated: as a single pixel at an instantaneous point of time, a pixel time series demonstrating the time evolution of a fire throughout the day and as a pixel array at an instantaneous point in time. The first two techniques had mixed results in achieving neural network convergence, however the third, a spatial technique consisting of 7x7 pixel arrays with the hottest part of the fire as the central pixel, was successful. In the 4 micron band, the approximate location of hot spots were identified by the NOAA's fire product, then the local minima technique identified the hottest part of the fire. In all 3 bands, using the image coordinates of the hottest fire pixel, pixel arrays of size 7x7 were collected around that central point. A typical spatial fire pattern for the MODIS sensor is shown in Table 3. Numeric values represent reflectance or brightness temperature scaled to a 0 – 255 range. In the 3.96 μm band the pattern becomes visually obvious. Moving away from the central pixel, the cooler parts of the fire are represented by rising intensity values (an inversion by design).

4. Neural Network Architecture

Three bands of 7x7 pixel arrays, formatted as 147 element vectors determined the number of network input nodes while the number of hidden nodes was initially determined by the rule-of-thumb to start with the square root of the sum of the inputs

Table 3. Typical 3 Channel MODIS 7x7 Pixel Array Spatial Fire Signature

CH1 (0.66 μm)

70	65	65	73	74	71	66
81	76	80	68	67	61	63
74	75	74	75	75	61	62
63	71	80	81	79	66	63
62	69	77	78	77	69	59
69	75	69	78	77	67	72
85	82	65	69	67	72	79

CH2 (0.86 μm)

139	156	155	125	133	135	145
151	143	141	129	129	137	142
146	143	143	136	129	145	142
144	146	128	127	128	138	142
148	144	138	124	125	134	145
140	145	147	123	123	138	131
129	136	148	141	144	146	136

CH22 (3.96 μm)

46	51	48	35	35	38	48
41	38	35	41	43	51	50
46	41	34	20	42	53	52
52	21	3	0	21	51	51
51	36	4	28	43	49	56
41	42	50	48	41	49	42
28	35	47	47	49	43	37

and outputs, i.e.12. Even with some experimentation though, the number of hidden nodes did not vary much from the initial value. A single output node was required to discriminate between the 2 classes. The 147-10-1 supervised, feedforward backpropagation neural network configuration used for training and testing is shown in Figure 3. Separate, identical networks were created for each sensor. Hyperbolic tangent transfer functions were selected for all active nodes.

Defining equations of the network for levels 0, 1 and 2 can be simply expressed by the following notation:

$$O_i^0 = I_i^0 \qquad I_j^1 = \sum_{i=1}^{N} W_{j,i}^{i+1} O_i^0 \qquad O_j^1 = f(I_j^1)$$

$$I_1^2 = \sum_{j=1}^{N} W_{1,j}^{h+1} O_j^1 \qquad O_1^2 = f(I_1^2)$$

where:

I = Induced Local Field
O = Nodal Output
I, O superscripts = layer number
I, O subscripts = node index number
W = connectionist weight
W superscripts = destination layer
W subscripts = destination and source node index numbers, respectively
N = total number of nodes per layer
i = input node index number (1 to 147)
h = number of hidden nodes (10)
j = hidden node index number (1 to 10)
f = tanh(x)

Figure 3, 147-10-1 MODIS, GOES or AVHRR FFBP NEURAL NETWORK

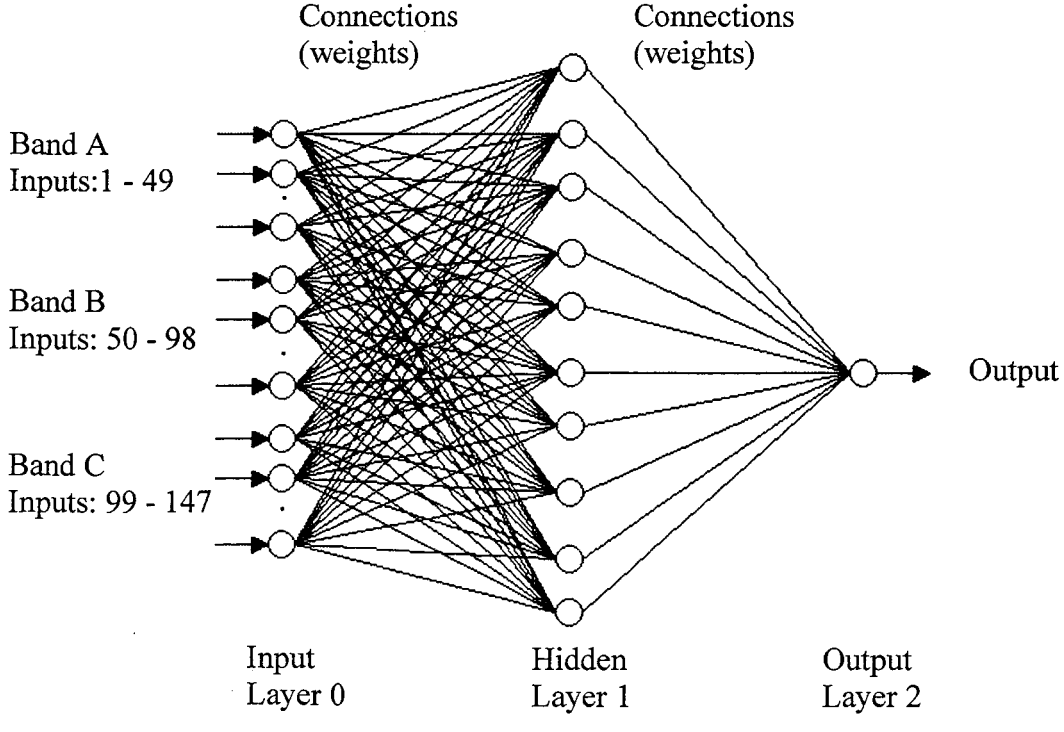

5. Neural Network Training and Testing

Thousands of spatial pattern training samples were extracted from the 3 sensor imagery which temporally spanned the 2003 fire season across the continental United States. Three different neural network modeling tools were used in the course of the investigation: Java Object Oriented Neural Engine (JOONE), Stuttgart Neural Network Simulator (SNNS) and MATLAB Neural Network Toolbox however the following discussion pertains only to results obtained with the MATLAB tool.

For each of the satellite instruments/sensors, the total available samples of spatial patterns extracted from satellite imagery is shown in Table 3, the ratio of fires to nonfires being approximately 1:1. A variation of the cross-validation technique [4] was employed for training and testing. Total available patterns for each instrument were divided into 4 quarters, each being representative of the entire data set. Training samples constituted ½ of the total number of patterns with ¼ relegated to a validation set and ¼ a test set resulting in 3 disjoint data sets. Batch training using the Gradient Descent with Momentum algorithm was selected from a suite of the available MATLAB routines and to prevent overfitting, early stopping was employed (though not in all cases). During training, the mean squared error on the validation set was monitored and when it began to rise, training was automatically halted. Testing then continued on data that had not been seen by the neural network during the training phase.

Table 3 Total Available Samples

MODIS	AVHRR	GOES-EAST	GOES-WEST
25,713	43,758	73, 010	53,922

5. Classification Results

Results of the neural network classification for MODIS, AVHRR and GOES data are presented below in the form of error matrices in Tables 4 – 7 (see Congalton's excellent discussion [5]). Analysis of the error matrices is discussed in the next section. Since this is a 2-class system, empirical data represents true positives (TP), true negatives (TN), false positives (FP) and false negatives (FN) which occupy the upper left hand corners of the error matrices. Remaining numeric data shown in the matrices are marginal totals.

Table 4 MODIS Error Matrix

		Reference Data		
		Fire	NonFire	
Classified Data	Fire	2834 (TP)	173 (FP)	3007
	NonFire	318 (FN)	3103 (TN)	342
		315	3276	6428

Table 5 AVHRR Error Matrix

Classified Data	Reference Data: Fire	Reference Data: NonFire	
Fire	5500	479	597
NonFire	624	4336	496
	6124	4815	10930

Table 6 GOES-WEST Error Matrix

Classified Data	Reference Data: Fire	Reference Data: NonFire	
Fire	4826	771 (FP)	5597
NonFire	1451	6432	7883
	6277	7203	13480

Table 7 GOES- EAST Error Matrix

Classified	Reference Data: Fire	Reference Data: NonFire	
Fire	7445 (TP)	2304 (FP)	9749
NonFire	1312 (FN)	7191 (TN)	8503
	8757	9495	18252

5. Statistical Analysis

The error matrices of Tables 4 – 7 were analyzed statistically in the manner of Congalton et al. [5] with results tabulated in Table 8. In terms of true positives (TP), true negatives (TN), false positives (FP) and false negatives (FN), 5 measures of accuracy were calculated as follows:

Overall Accuracy	(TP+TN)/(TP+TN+FP+FN)
Producer's Accuracy (fire)	TP/(TP+FN)
Producer's Accuracy (nonfire)	TN/(FP+TN)
User's Accuracy (fire)	TP/(TP/FP)
User's Acuracy (nonfire)	TN/(TN+FN)

This was followed by a Kappa analysis [5] in which the Khat statistic determines the degree of agreement between classified data and reference data. The Overall Accuracy measure reflected the neural networks ability to assign unknown image pixels to either of two classes, fire and background while the Producer's and User's Accuracy figures provided accuracy measures for individual classes. As Table 8 indicates, a high degree of classification accuracy (~90% Overall and 87% – 94% Producer's/User's) was achieved for the MODIS and AVHRR sensors while classification of GOES image data (mid 70% – mid 80%) performed relatively poorly. This was attributed to the accuracy of the science instruments themselves as well as the refinement in fire detection algorithms which followed the earlier GOES methods. KHAT values which have a range of +1 to -1 indicated positive correlations in all cases while MODIS and AVHRR classifications achieved a strong agreement (greater than 80%) and GOES (low to mid 60% range) again lagged behind.

Table 8 Statistical Analysis of Neural Network Classification

STATISTIC	MODIS	AVHRR	GOES WEST	GOES EAST
Overall Accuracy	92.3615	89.9168	83.5163	80.1885
Producers Accuracy (fire)	89.9112	89.8106	76.8839	85.0177
Producers Accuracy (nonfire)	94.7192	90.0519	89.2961	75.7346
Users Accuracy (fire)	94.2468	91.9886	86.2248	76.3668
Users Accuracy (nonfire)	90.7045	87.4194	81.5933	84.5702
Khat	0.847041	0.796063	0.666441	0.60486

6. Conclusions

The original intent of the project was to develop a single neural network that could process sensor data from all 3 instruments, MODIS, AVHRR and MODIS, perform fire classification at least as well as the automated algorithms and human fire analysts currently achieve and be incorporated into NOAA's operational Hazard Mapping System to reduce the amount of manual intervention. Our research has shown that there was insufficient temporal and spatial overlap between the 3 sensors to process image data with a single network nor would it have been practical at any rate due to the extraordinary network size which was exacerbated by the 7x7 pixel arrays to characterize fire patterns. The practical solution was to divide processing between 3 independent networks however the low classification accuracy for GOES EAST and GOES WEST imagery suggests that only MODIS and AVHRR imagery need be processed by the neural network. In spite of the high classification accuracy that was achieved for MODIS and AVHRR sensor data, further improvement is likely to be achieved by incorporating additional generalization techniques that MATLAB offers: Modified Performance Function, and Bayesian regularization. Further research effort is still required before the neural designs could be incorporated into an operation al system.

7. References

[1] D.McNamara, G. Stephens, M. Ruminiski, NOAA's multi-sensor fire detection program using environmental satellites, Earth System Monitor, Vol. 13, No.1, September 2002.

[2] D. McNamara, G. Stephens, B. Ramsay, E. Prins, I. Csiszar, C. Elvidge, R. Hobson, and C. Schmidt, Fire detection and monitoring products at the national oceanic and atmospheric administration, Journal of the American Society for Photogrammetry and remote sensing, Volume 68, Number 8, August 2002.

[3] National Aeronautics and Space Administration, 2000, MODIS data products catalog (EOS AM platform): [Greenbelt, Maryland], Goddard Space Flight Center, http://modis.gsfc.nasa.gov.

[4] S. Amari, N. Murata, K. –R., Muller, M. Finke, H.H. Yang, Asymptotic Statistical theory of overtraining and cross-validation, IEEE Transactions on Neural Networks, Volume8, Pages 985 – 996, September, 1997.

[5] R. G. Congalton, K. Green, Assessing the Accuracy of Remotely Sensed Data: principles and Practices, 1999.